Laser beam welding of CuZn open-cell foams

C.A. Biffi [a,*], D. Colombo [b], A. Tuissi [a]

[a] National Research Council CNR, Institute for Energetics and Interphases, Unit of Lecco, C.so Promessi Sposi 29, 23900 Lecco Italy
[b] Politecnico di Milano, Mechanical Engineering Department, Via La Masa 1, 20156 Milano, Italy

Article history:
Received 10 March 2014
Received in revised form
31 March 2014
Accepted 12 May 2014
Available online 17 June 2014

1. Introduction

Cellular materials are an innovative and challenging class of materials that can offer an interesting and seemingly unique combination of morphological and material characteristics [1]. Therefore, the interesting physicochemical and mechanical properties of these materials make them very attractive for both structural and functional applications in different sectors. Different processes can be used to produce cellular materials. One concern, however, is the infiltration of leachable solid particles into the molten alloy [1–4]. The most studied metallic foams in the literature are generally Al-based alloys obtained via the liquid infiltration of leachable space holders because of their light weights, high stiffness, good thermal stabilities, and low manufacturing costs [4]. The formation of open-cell foams using silica gel as a space holder was proposed for CuZnAl and CuZn alloys [5–6]. The functional response of these foamed alloys has considerable potential; CuZnAl alloy foams show both interesting shape memory effects and pseudo-elasticity [7–8] in a lighter structure with no significant degradation in these properties relative to the initial material. The effect of mechanical cycling of CuZnAl alloy foams, on the order of a few hundred cycles, was also investigated at different temperatures, and the results indicated that their functional performance exhibited good stability [9].

This potential for these foams makes their processing an important issue for increasing their applications [10]. Some studies have reported on the use of laser beams, for assisting the foaming process [11], for bending [12], for cutting [13], and for welding [14] foams, which usually have pores size on the micro scale. The most important factor for foams is their pore size, which can affect both the final foam performance and the process performance. Specifically, larger pores lead to more potential foam applications; for example, foams with porosities on the order of a few millimetres can be used as the active elements in heat exchangers [15]. A practical problem for this application is joining the foams to other elements or structures to produce more complex systems; for these reasons, the authors proposed to investigate the joining of Cu-based alloy foams using laser technology.

The objective of this work is to investigate the process of fibre laser welding open-cell $Cu_{60}Zn_{40}$ [wt%] brass foams using a 1 kW

* Corresponding author.
E-mail address: carlo.biffi@ien.cnr.it (C.A. Biffi).

continuous-wave (CW) fibre laser. These foams, with a pore size of approximately 3.5 mm $\pm$ 0.5 mm, were produced using a vacuum induction melting system via the liquid infiltration method with silica gel as the space holder. The space holders used to generate the pores were subsequently removed via chemical etching. A peculiar characteristic of foams produced via this method is their open-cell structure, which ensures the interconnection of adjacent pores [5,6].

Some preliminary welding tests were performed with the foams in a bead-on-plate configuration; however, weld beads were not obtained because of the large pore size relative to the laser beam and because of the high porosity of the foams (approximately 66%). However, the laser welding process was successfully performed in the lap joint configuration, in which a thin plate of the same material was placed on the top of the foam surface. The effect of the process speed (5–20 mm/s) on the geometrical characteristics of the transverse sections of the joints was studied and the heat-affected zone (HAZ) was identified using the microhardness profile. Compositional analyses of the weld bead and HAZ were also performed using a scanning electron microscope (SEM) coupled with an energy dispersive spectrometer (EDS). Therefore joining of high-reflectivity porous alloys with complex structures and pore sizes on the order of several millimetres was proved using a CW fibre laser in the lap joint configuration.

2. Experimental

Ingots (60 mm in diameter) of $Cu_{60}Zn_{40}$ [wt%] brass were melted in an Aseg Galloni VCMIII induction melting system under a pure Ar flow. The material was then foamed via the liquid infiltration method using amorphous SiO_2 spheres (Sigma S7500 Type II) as space holders. The process details have previously been described elsewhere [5,9]. After foaming, the SiO_2 particles were removed via chemical etching (50% HF and 50% H_2O). A typical section of the foam is shown in Fig. 1a nearly round, interconnected pores are clearly visible. An average pore fraction of 65–70% was calculated via image analysis and weight/volume measurements.

The welding process was performed using a CW fibre laser (mod. YLR 1000 from IPG Photonics). The primary characteristics of this laser is shown in Table 1.

After preliminary tests in a bead-on-plate configuration, experiments of joining the foams were performed using the lap joint configuration, in which the foams were joined to a 1-mm-thick cold rolled plate of the same material that was placed on the top surface of the foam (Fig. 1b). During these experiments, the welding speed was varied across the range from 5–20 mm/s, and three replicas were performed for each of the tested welding condition. A summary of the employed process parameters is presented in Table 2. Fig. 2 shows the multi-nozzle system that was used to cover the weld beads with a sufficient argon flow during the laser joining process; this device was designed to minimise the evaporation of Zn due to its low melting and boiling points.

The weld beads were mechanically sectioned, and their metallographic cross sections were prepared and analysed using optical microscopy (OM) and SEM. Microhardness tests were performed both on un-welded samples for the hardness characterisation of the base material and on the welded ones to obtain the hardness profile across the weld bead and the HAZ as a function of the process speed. Moreover, a compositional analysis was performed using EDS to evaluate any chemical changes in the proximity of the laser joint.

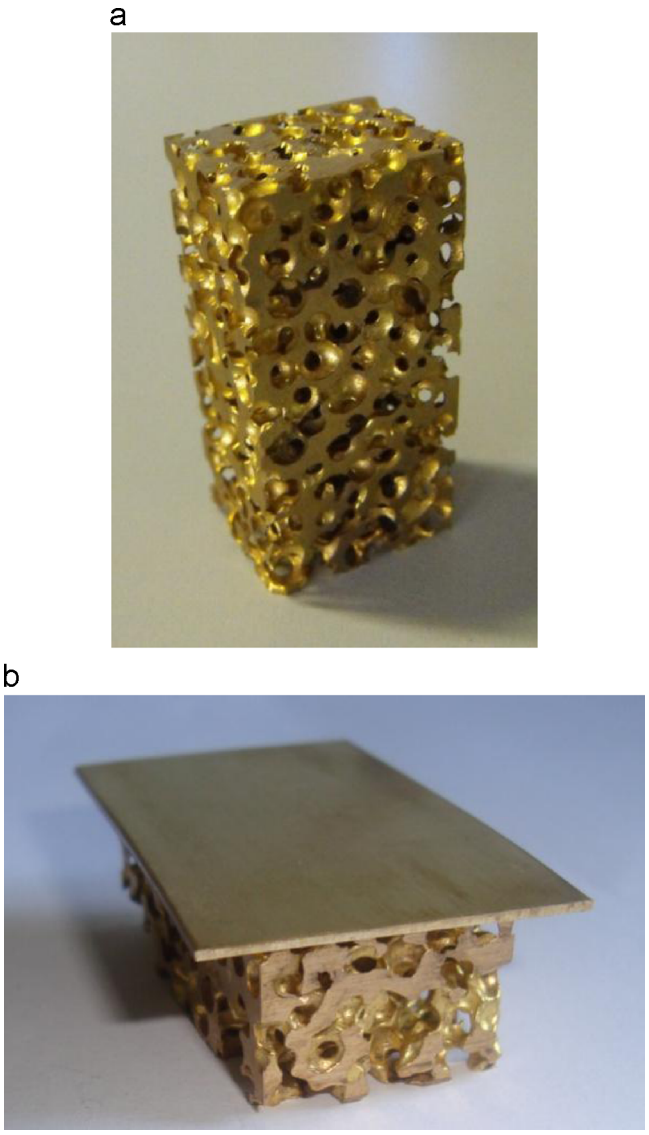

Fig. 1. Representative section of the foam (a) and lap joint configuration used for the welding test (b).

Table 1
Main characteristic of the fibre laser, used in the welding experiments.

Maximum power (W)	1000
Modality od laser emission	CW-QCW
Laser central wavelength (nm)	1070
Beam quality factor	5.14
Diameter of the process fibre optics (μm)	50

3. Analysis and discussion of the results

Laser welding the foams in a bead-on-plate configuration was first attempted for preliminary evaluation of the laser welding process. According to the result shown in Fig. 3, welding cannot be successfully achieved in the absence of a filler material because the pore size of the cellular material is significantly larger than that of the laser spot and because there are very few contacts between the materials to be welded. Therefore, in order to ensure a constant laser-material interaction, the laser joining process was

investigated in a lap joint configuration by placing a thin plate of the same alloy on the top surface of the foam (Fig. 1).

Fig. 4 shows a cross section of a bead welded in the lap joint configuration at 10 mm/s. In this picture, the difference between the size of the weld bead produced by the fibre laser and the pore size inherent to the investigated foams is apparent. This difference indicates that joining cellular structures requires a material to be added to obtain a weld bead and to avoid destroying the foam structure (Fig. 3).

Fig. 5 shows representative cross sections of weld beads obtained at process speeds from 5 mm/s to 20 mm/s with a power of 1 kW in the lap joint configuration. The thin plate material partially falls into the cellular structure, which allows it to join with the substrate. Joining of the thin plate and foam only occurred where the cellular structure presented a pore border; without a pore border, the connection cannot occur. Moreover, no cracks were observed in either the weld bead or in the HAZ.

The bead penetration clearly varies as a function of the cellular structure morphology encountered by the laser beam. For this reason, the bead penetration measurements do not appear to be representative of this investigation; therefore the weld bead width was measured at half of the thickness of the plate as a mean indicator of the weld bead size.

Fig. 6 shows the interval plot for the weld bead width at the analysed welding speeds; for each welding speed the sample mean value is represented by the black dots while each single bar around the mean represents its 95% confidence interval (CI).

A significant reduction in the width of the weld beam is observed from a mean value of 0.58 mm to 0.36 mm, which is directly associated with increasing the process speed because of the decreasing specific energy density. As for the process variance, a relatively high 95% CI for the mean is observed at all the welding speeds. Similarly to the weld bead penetration, this result can be partially related to the inhomogeneous morphology of the cellular structure of the foam.

Another representative variable that is characteristic of the weld beads is the HAZ.

The analysis of the micrographs in Figs. 4 and 5 show that a microstructure variation of the material is hard to be observed near the molten zone. This phenomenon can be mainly related to the fast thermal cycle of the laser welding process itself that, in conjunction with the high thermal conductivity of the copper inside the welded samples, does not allow for a significant variation of the sample structure.

Table 2
Variable and fixed process parameters, used in the welding experiments.

Variable parameter	Process speed	5–10–15–20 mm/s
Fixed parameters	Power	1000 W
	Laser spot	0.54 mm
	Assist gas	Argon
	Gas pressure	5 bar
	Gas flow	40 l/min
	Inclination of the laser beam	10°
	Collimation length	100 mm
	Focusing length	200 mm
	Focal position	+3 mm

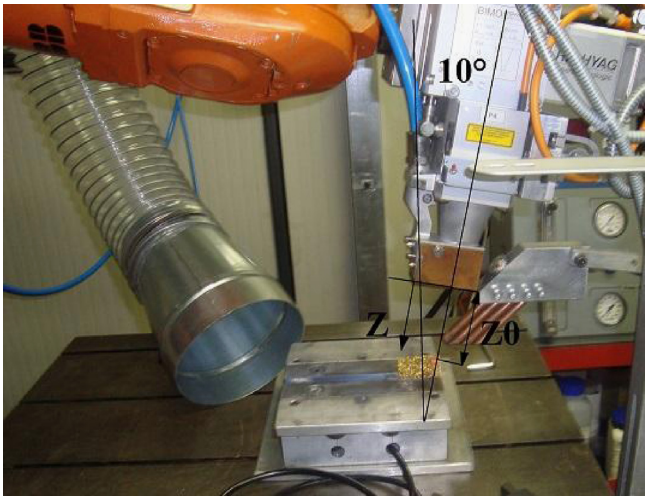

Fig. 2. Nozzle system for covering the welding with the assist gas.

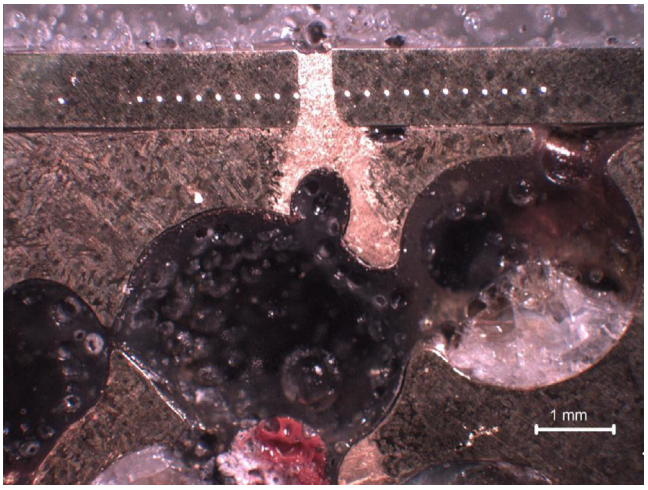

Fig. 4. Representative micrograph, at low magnification, of the welded bead in lap joint configuration (process speed 10 mm/s).

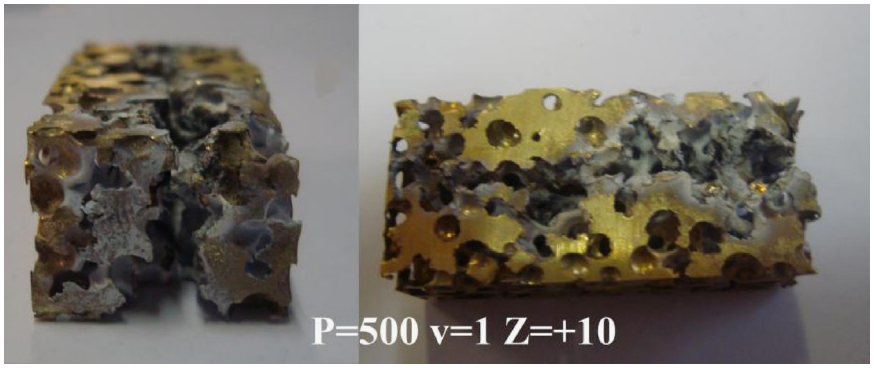

Fig. 3. Representative trial of laser welding in a bead on plate configuration.

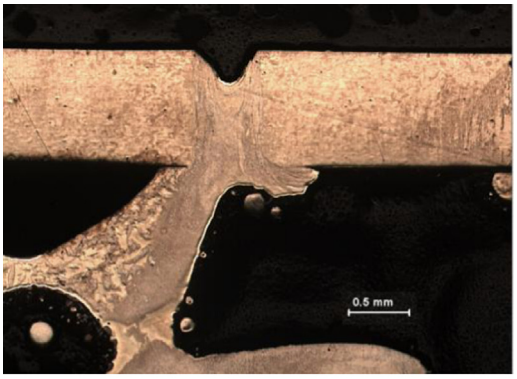

V=5 mm/s

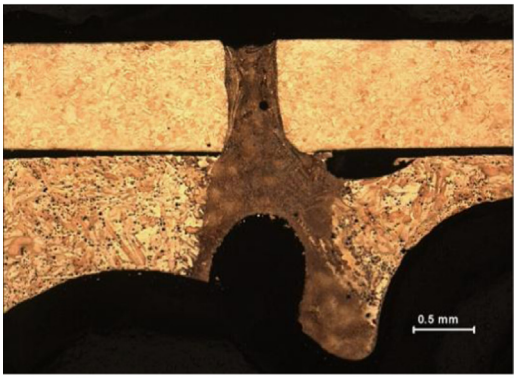

V=10 mm/s

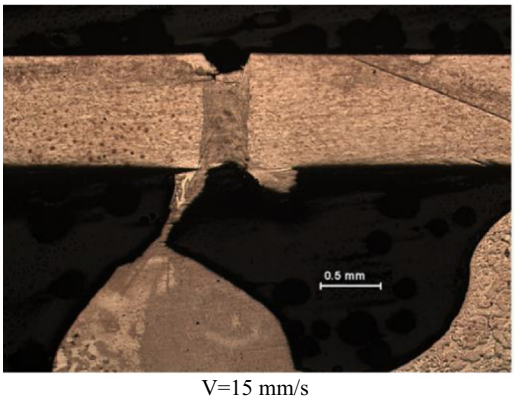

V=15 mm/s

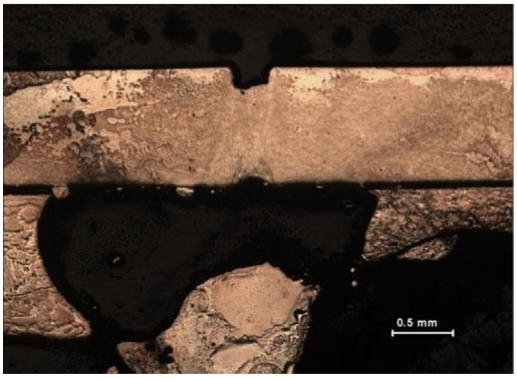

V=20 mm/s

Fig. 5. Micrographs of the welded bead, at varying the process speed, in the lap joint configuration.

However, because of the cold rolled condition of the plates, a relief of the internal stresses of the welded plates was expected leading to lower hardness where this relief occurs.

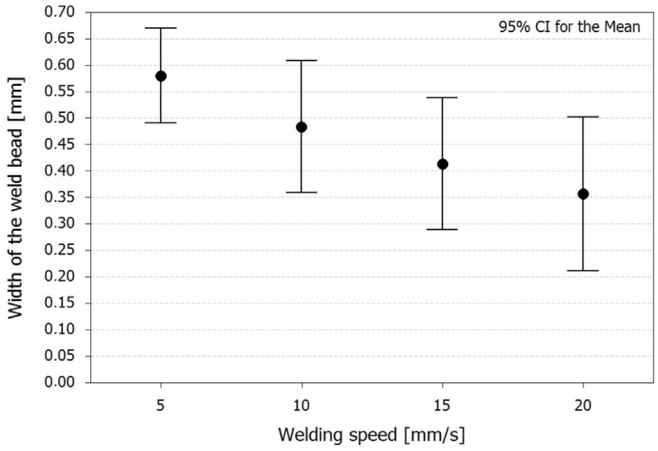

Fig. 6. Interval plot for the width of the welded bead in function of the process speed.

Therefore the HAZ was considered as the extension of the zone near the weld bead where an hardness value lower than the one of the base material is observed, by evaluating the microhardness profile across the weld bead at half of the thickness of the thin plate (as shown in the indentation in Fig. 4).

The micro hardness analysis was performed for the two most relevant welding condition, such as the one related to the lowest welding speed of 5 mm/s and the one at the highest welding speed of 20 mm/s, as shown in Fig. 7.

The distribution of the hardness value for the base material was evaluated by performing three HV0.2 hardness measurements for the three replica of both the two welding speed conditions leading to a total of 18 measurements. A mean hardness value of 90.1 HV with a 95% CI between 89.1 HV and 91.0 HV was calculated for the base material, as described in [16].

The microhardness trend at welding speed of 5 mm/s is shown in Fig. 7a the mean hardness trend is represented by the black dots, while for each x [mm] position the estimated 95% CI of the three sampled replica is represented by the vertical bars, whose higher extension in comparison to the CI of the base material is related to the lower sampling dimension [16].

The centre of the weld bead exhibited the highest hardness (approximately 125–130 HV); rapid solidification due to the high cooling speeds characteristic of laser welding usually generates a fine microstructure with a higher hardness value. Thus, a significant reduction in the hardness was detected from the melted zone (MZ) to the HAZ. This softening appears to occur in the HAZ even if the hardness variation between the HAZ and BM is limited but still present. The extent of the HAZ was estimated as the distance above which the hardness had stabilised to the value of the base material; therefore for samples welded at the minimum process speed (Fig. 5a), the complete HAZ width, including the melted material, was approximately 4 mm.

Fig. 7b shows the hardness profile measured for the weld bead produced at the highest process speed (20 mm/s). In this case a relatively shorter HAZ of 3.5 mm (including the melted material) is observed, even if a similar softening effect of the 5 mm/s welding condition is reported in terms of hardness reduction.

Because of that the extent of the HAZ, ranging from 4 mm (welding speed of 5 mm/s) to 3.5 mm (welding speed of 20 mm/s), does not appear to be strongly influenced by the investigated process speeds.

Finally, a compositional analysis was performed in the proximity of the weld bead produced at a process speed of 5 mm/s. Fig. 8 shows the area selected for these EDS measurements, a table

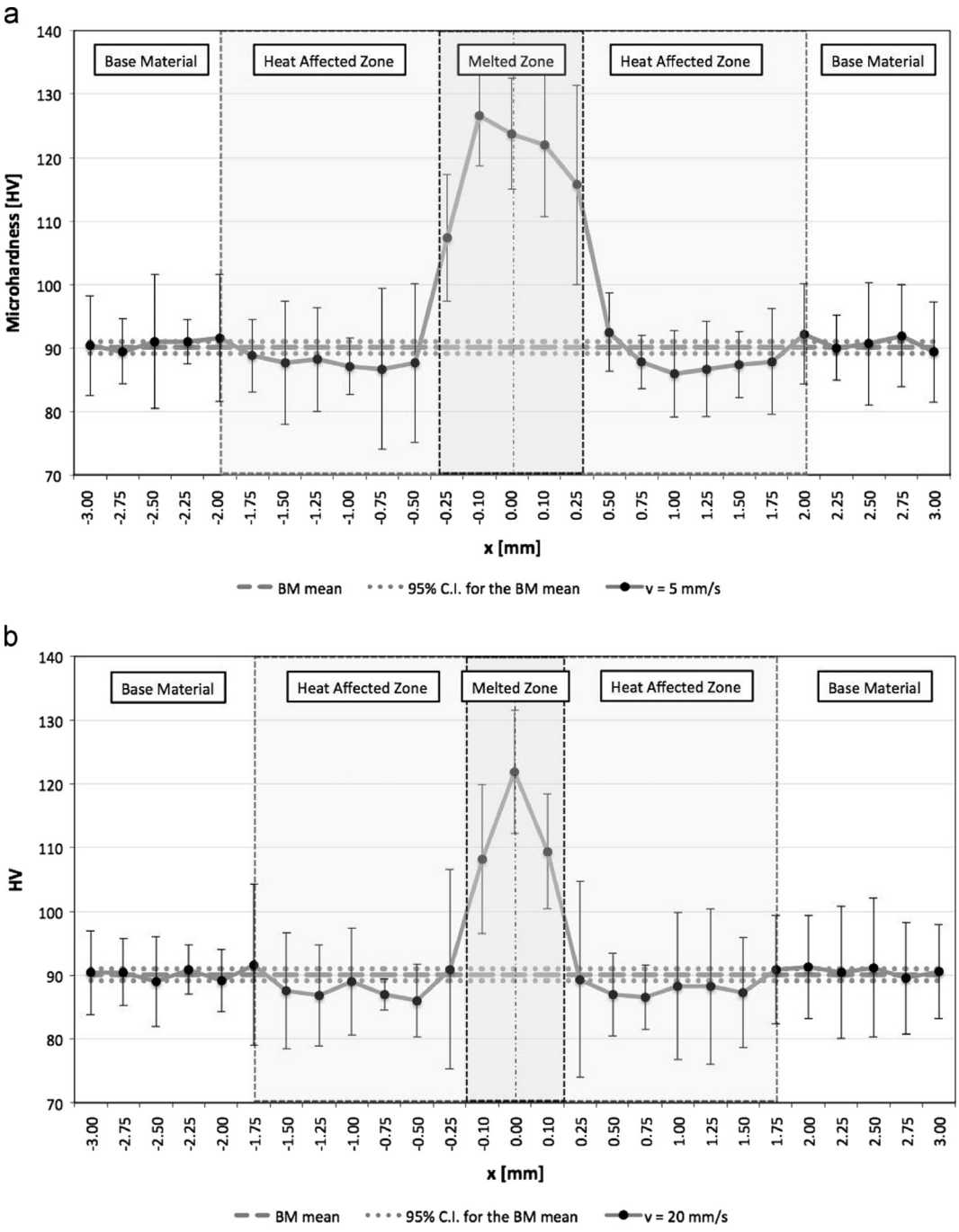

Fig. 7. Microhardness across the welded beads, performed at 5 mm/s (a) and 20 mm/s (b),respectively.

containing the elemental contents and two representative spectra for the BM and MZ. No significant modification in the chemical composition was detected; the loss of Zn, which is characterised by low melting and boiling points, was avoided [17], most likely due to the shielding provided by the assist gas.

4. Conclusions

In this work, a welding process using a 1 kW continuous-wave fibre laser was studied using open-cell $Cu_{60}Zn_{40}$ [wt%] brass foams. Following some preliminary welding tests in the bead-on-plate configuration that yielded poor results, the joining process was successfully performed in the lap joint configuration. The following main conclusions were drawn:

- Weld beads were obtained via the connection between the plate and some of the foam pores. Melted material from the thin plate was necessary for joining the plate to the foam because it fell into the gaps of the bulk cellular materials. No cracks were observed in the proximity of the weld bead.
- The process speed influenced the extent of the MZ but only slight variation are observed in the case of the HAZ. The mean width of the weld bead ranged between 0.36 and 0.58 mm, whereas the size of the HAZ, including the width of the weld

a

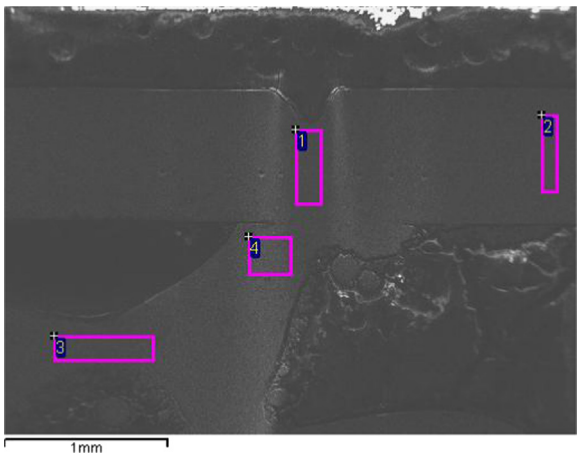

b

EDS area	Material condition	Cu [%wt]	Zn [wt]
1	MZ	61	39
2	BM	62	38
3	BM	58	42
4	MZ	60	40

c

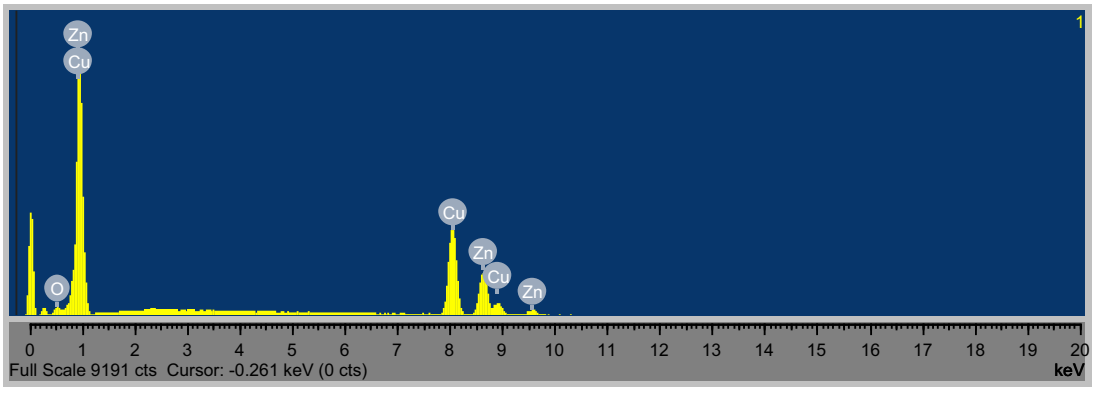

d

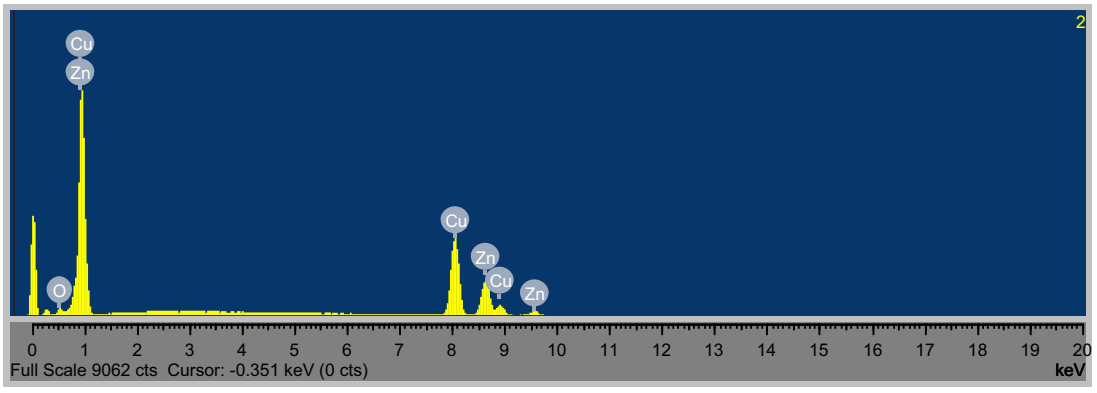

Fig. 8. Zone of EDS measurements (a), compositional analysis (b) and representative spectra of the welded bead (c), performed at 5 mm/s, and of the base material (d).

bead, was estimated to be approximately 4 mm for the lowest speed and 3.5 mm for the highest speed.

- The hardness profile showed that the mechanical properties of the material increased from a mean value of 90.1 HV (BM) to 125–130 HV (MZ). The HAZ softened, which was most likely dependent on the cooling rate.
- The compositional analysis did not reveal any significant modification to the material chemistry. The thermal cycle

imposed by the laser beam did not reduce the Zn content, which was the potentially problematic element due to its low melting and boiling points. The assist gas flow produced a shielding effect that properly covered the weld bead.

This study demonstrated that welding using a fibre laser can be employed for joining Cu-based foams. Weld beads were obtained in the lap joint configuration as a result of material falling from the thin plate to fill the pore voids.

Acknowledgements

The authors wish to thank Prof. Barbara Previtali, Eng. Andrea Panzeri, Mr. Marco Pini, Mr. Nicola Bennato, and Mr. Giordano Carcano for their support during these experiments. This work was developed in the framework of the “Matec” project.

References

[1] Ashby MF, Evans A, Fleck NA, Gibson L, Hutchinson JW, Wadley H. Metal Foams: A Design Guide. Boston: Butterworth-Heinemann; 2000.
[2] Banhart J. Manufacture, characterization and application of cellular metals and metal foams. Prog Mater Sci 2001;46:559.
[3] Wadley HNG. Cellular metals manufacturing. Adv Eng Mater 2002;4:726.
[4] Despois JF, Marmottant A, Salvo L, Mortensen A. Influence of the infiltration pressure on the structure and properties of replicated aluminium foams. Mater Sci Eng A 2007;462:68.
[5] Castrodeza EM, Mapelli C, Vedani M, Arnaboldi S, Bassani P, Tuissi A. Processing of shape memory CuZnAl open-cell foam by molten metal infiltration. JMEPEG 2009;18:484–9.
[6] Castrodeza EM, Mapelli C. Processing of brass open-cell foam by silica-gel beads replication. J Mater Process Technol 2009;209:4958–62.
[7] Bertolino G, Larochette P, Castrodeza EM, Mapelli C, Baruj A, Troiani HE. Mechanical properties of martensitic Cu–Zn–Al foams in the pseudo-elastic regime. Mater Lett 2010;64:1448–50.
[8] Arnaboldi S, Bassani P, Passaretti F, Redaelli A, Tuissi A. Functional characterization of shape memory CuZnAl open-cell foams by molten metal infiltration. JMEPEG 2011;20:544–50.
[9] Tuissi A, Bassani P, Biffi CA. CuZnAl shape memory alloys foams. Adv Sci Technol 2013;78:31–9.
[10] Seeliger H-W. Manufacture of aluminum foam sandwich (AFS) components. Adv Eng Mater 2002;4–10:753–8.
[11] Kathuria YP. A preliminary study on laser assisted aluminum foaming. J Mater Sci 2003;38:2875–81.
[12] Guglielmotti A, Quadrini F, Squeo EA, Tagliaferri V. Laser bending of aluminum foam sandwich panels. Adv Eng Mater 2009;11:902–6.
[13] Yilbas BS, Akhtar SS, Keles O. Laser hole cutting in aluminum foam: influence of hole diameter on thermal stress. Opt Lasers Eng 2013;51:23–9.
[14] Bernard, T., Burzer, J., Bergmann, H.W., Mechanical properties of structures of semifinished products joined to alluminium foams, 115 (2001) 20–24.
[15] Biffi, C.A., Tuissi, A., Thermo-fluid dynamic modeling of Cu based metallic foams for heat exchanger applications, In: Proceedings of the COMSOL Conference, Rotterdam 23-25/10/2013.
[16] Montgomery DC, Runger GC. Applied Statistics and Probability for Engineers. 3rd editionJohn Wiley and Sons; 2003.
[17] Biffi CA, Bassani P, Tuissi A, Carnevale M, Lecis N, LoConte A, et al. Flexural vibration suppression of glass fibre/CuZnAl SMA composite. Funct Mater Lett 2012. http://dx.doi.org/10.1142/S1793604712500142.